

# Characteristics of Tropospheric Ozone Pollution and Analysis of the Influencing Factors in the Horqin Grassland

Jinyang Wang<sup>1,2</sup>, Tianzhen Ju<sup>1,2,\*</sup>, Bingnan Li<sup>3</sup>, Shuai Peng<sup>1,2</sup>, Shengtong Lei<sup>1,2</sup>

<sup>1</sup>College of Geography and Environmental Sciences, Northwest Normal University, Lanzhou, Gansu, 730070, China

<sup>2</sup>The Key Laboratory of Resource Environment and Sustainable Development of Oasis, Lanzhou, 730000, China

<sup>3</sup>Faculty of Atmospheric Remote Sensing, Shaanxi Normal University, Xi'an, 710062, China

\*Corresponding author: jutianzhen@nwnu.edu.cn

**Abstract:** This study used the daily product data of atmospheric tropospheric column ozone concentration collected by Aura Satellite Ozone Monitor (OMI). Image-based spatial analysis, theta-slope trend index, Hurst index and Pearson correlation analysis were used to evaluate the ozone pollution status in the Horqin Grassland region. It was found that the column ozone concentrations showed an overall increasing distribution from west to east, with the lowest concentration in 2014 and the highest in 2019. The Slope Trend Index and the Hurst Index showed that the concentration values are slightly increasing and may increase with the region's future development. The study of factors affecting ozone concentration found that precipitable water and temperature have a more significant effect on ozone.

**Keywords:** Tropospheric ozone; OMI; Slope; Hurst index; Horqin grasslands region

## 1. Introduction

Ozone (O<sub>3</sub>) is produced by a series of atmospheric photochemical reactions of precursors such as volatile organic compounds (VOCs) and nitrogen oxides (NO<sub>x</sub>) in the presence of ultraviolet light. High concentrations of ground-level ozone increase urban photochemical smog pollution. It is a secondary pollutant with oxidizing solid properties. Strongly irritating to eyes and respiratory tract. It impairs human lung function and even leads to various diseases (Tang et al., 2006). It is harmful to the human respiratory system and skin organs. At the same time, its oxidizing solid properties can cause various degrees of damage to buildings, plants, and animals. It can cause damage to the earth's ecology and human society with different degrees of influence. (Liu, 2008)

Since the occurrence of photochemical smog in Los Angeles in the 1840s, ozone has attracted widespread attention abroad, and a series of studies have been conducted around the formation and transport of ozone. Especially in the Houston area of the United States, where numerous oil refineries and chemical plants are distributed, there are numerous chemical plants with severe ozone pollution (Senff et al., 2010; Pan et al., 2017). With the rapid economic development and urbanization in China. Compound atmospheric pollution, represented by atmospheric ozone and delicate particulate matter, is becoming increasingly severe (Hu et al., 2009). Domestic scholars have carried out a large number of studies on ozone pollution. Since the 1990s, Tang et al. (Zhang et al., 1998; Jiang et al., 2001; Yin et al., 2004; Shan et al., 2006; Qu et al., 2009; Xie et al., 2009) have studied the changing patterns of O<sub>3</sub> and related influencing factors in different types of cities. The Institute of Atmospheric Physics (IAP) of the Chinese Academy of Sciences analyzed the monthly mean and seasonal variations of ozone concentrations in the boundary layer of Beijing based on O<sub>3</sub> sounding data (Zong et al., 2007). Wang et al. (2009) quantified the contribution of emissions from different regional sources to ozone pollution in the peri-urban areas of Beijing by using the ozone source identification technique and the regional ozone assessment technique. Deng et al. (2011) found that the average ozone values in the PRD were higher in spring, summer, and autumn. Ozone maxima exceeding 120 ppb often occur in spring and summer. Air pollution observations by Xu et al. (Xu et al., 2006; Zhu Shuai et al., 2006) showed that high concentrations of O<sub>3</sub> have been observed in the Yangtze River Delta region. Ran et al. (2011) investigated the sensitivity factors of ozone production in the North China Plain region using the NCAR-MM photochemical box model. The study showed that the region is a NO<sub>x</sub> control area, and ozone generation

is susceptible to VOC activity. Li et al. (2020) analyzed the sensitivity of atmospheric ozone production in Lanzhou City using the OZIPR model and made corresponding recommendations for reducing precursor emissions[1-5].

The existing research results show that many scholars' studies on ozone are concentrated in typical urban areas with dense populations and developed industries. The focus is on the sources and transport of ozone formation and gradually combined with the interaction of delicate particulate matter to explore the mechanism, prevention, and control of complex air pollution. Studies have yet to be conducted in arid and semi-arid grassland areas such as the Inner Mongolia Autonomous Region, where natural conditions dominate. This paper focuses on the impact of biogenic emissions on regional ozone in the Horqin grassland area. In this way, we explore the regional differences in ozone emissions and provide some ideas for the response of ozone to biogenic and industrial emissions. It also provides some references for the atmospheric control in the Horqin grassland study area.

## 2. Overview of the study area

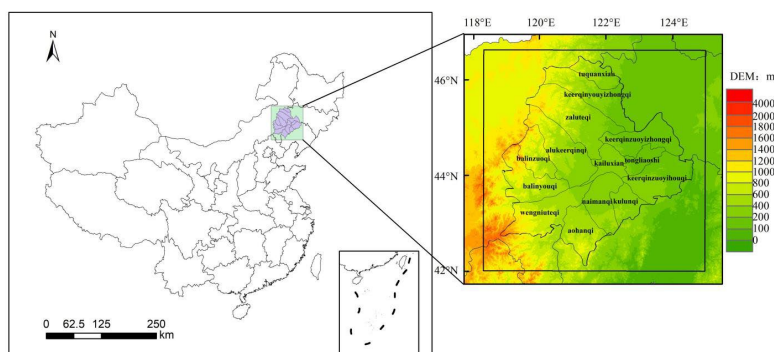


Figure 1: Overview of the Horqin grassland study area superimposed by the digital elevation model

The study area is the horqin sandland located in northern China's eastern part of the semi-arid agro-pastoral zone. The area is located at the intersection of three major transition zones: the Northeast Plain and the Inner Mongolian Plateau, the semi-humid and semi-arid, and the farming and animal husbandry. It lies roughly between 118°E-125°E and 42°N-47°N, with an average elevation of 476 m. Its location is shown in Figure 1. The Horqin sandland is one of the four significant sandlands in China. As a result of interference from human activities, the area of desertified land increased from 20% to 53% between the 1950s and the 1980s. The Horqin sandland belongs to the continental semi-arid and semi-humid monsoon climate. Spring is dry and windy. Summer is short and hot, with concentrated rainfall. Early frost in autumn, the temperature drops quickly. Winter is cold and long with little snowfall. The average annual temperature is 5.8-6.4°C, the annual precipitation is 343-451 mm, and the annual wind speed is 3.5-4.5 m/s.

## 3. Data sources and methods of analysis

In recent years, with the rapid development of satellite remote sensing, its application to various research fields is increasing. Using satellite remote sensing for monitoring and analyzing atmospheric pollutants better makes up for the small-scale range of ground monitoring and the weak advantages of regional analysis. Remote sensing satellite sensors used to monitor atmospheric pollutants are TOME, GOME, GOME-2, SCIAMACHY, and OMI(Lu et al., 2018). This paper uses the day-by-day data of tropospheric ozone column concentrations in the Horqin Grassland region from 2013 to 2020 from the Ozone Monitoring Instrument (OMI) on board the Aura satellite. It is stored in HDF5 format(Li et al., 2019; Curci et al., 2010; Lu et al., 2006). The correlation between OMI satellite data and ground data has reached more than 0.82 (Ma et al., 2020; Xu et al., 2021). The detector has a spatial resolution of  $0.25^\circ \times 0.25^\circ$ , a trajectory height of 705 km, and a wavelength range of 270-500 nm. Meteorological data were obtained from a dataset jointly provided by the National Centers for Environmental Prediction (NCEP) and the National Center for Atmospheric Research (NCAR). The dataset contains data from 1948 to the present[6-9].

Remote sensing data of daily column ozone concentrations in the study area for 2013-2020 were acquired to obtain data stored in HDFEOS strip (swath) data format. The data were then batch-processed

using VISAN3 and the python program. Latitude, longitude, pollutant column concentration, and cloudiness data were extracted using Python software. The coverage area of the pollutant column concentration in the study area was maximized by removing anomalies and fusing adjacent strip data. The spatial distribution map of pollutant concentration data in the Horqin grassland area with an accuracy of 0.01 image element was obtained by resampling the pollutant data in ArcGIS through format transformation, kriging spatial interpolation, averaging, and mask extraction.

### 3.1 Pearson correlation analysis

Pearson correlation analysis is used in this paper to analyze the spatial relationship between ozone and natural factors. The correlation coefficient  $r$  reflects the positive or negative correlation between variables and the degree of strength of the correlation (Huang et al. 2021).

$$r_{xy} = \frac{\sum_{i=1}^n (x_i - \bar{x})(y_i - \bar{y})}{\sqrt{\sum_{i=1}^n (x_i - \bar{x})^2 \sum_{i=1}^n (y_i - \bar{y})^2}} \quad (1)$$

Where:  $x$  and  $y$  represent two variables,  $r_{xy}$  is the correlation coefficient between the  $x$  and  $y$  variables, and  $i$  is the year number.

### 3.2 Pearson correlation analysis

In order to study the temporal and spatial trends of column ozone concentrations in the Horqin Grassland region over the past eight years. One-way linear regression analysis was used to establish the relationship between ozone column concentration and temporal changes. The spatial change characteristics of individual pixels at different times can be used to characterize the evolution of regional patterns in a specific time series (Peng et al. 2022). Formula (2) is calculated as:

$$\theta_{slope} = \frac{n \times \sum_{i=1}^n (i \times O_{3i}) - \sum_{i=1}^n i \sum_{i=1}^n O_{3i}}{n \times \sum_{i=1}^n i^2 - (\sum_{i=1}^n i)^2} \quad (2)$$

Where  $\theta_{slope}$  is the slope of each ozone column concentration value i.e., the coefficient of variation of the ozone column concentration for each pixel.  $i$  is the year for each of the years 2013-2020.  $n$  is the number of years from 2013 to 2020.  $O_{3i}$  is the specific ozone column concentration value corresponding to year  $i$ . When  $\theta_{slope} > 0$ , it indicates that the ozone column concentration also shows an increasing trend with time, When  $\theta_{slope} < 0$  then a decreasing trend is shown. The more significant absolute value of  $\theta_{slope}$  indicates that the magnitude of change in ozone column concentration values will be larger (Huang et al. 2019)[10-14].

### 3.3 Hurst Index

This paper uses the Hurst index to predict future trends in annual column ozone concentrations in selected regions of Horqin Grassland, which can quantitatively characterise the long-range dependence or persistence of a time series and help to analyse future trends at a particular time or space. This paper uses Matlab software to perform pixel calculations to determine the Hurst index.

The calculation is based on the following principle: located at moments  $t_1, t_2, \dots, t_n$ , the response time series obtained at  $\xi_1, \xi_2, \dots, \xi_n$ , and for any positive integer  $\tau \geq 1$ , the time series are averaged as (Wang et al. 2002):

The cumulative deviation is:

$$\langle \xi \rangle_{\tau} = \frac{1}{\tau} \sum_{t=1}^{\tau} \xi(t) \quad \tau = 1, 2, 3, \dots, n \quad (3)$$

$$X(t, \tau) = \sum_{t=1}^{\tau} (\xi(t) - \langle \xi \rangle_{\tau}), \quad 1 \leq t \leq \tau \quad (4)$$

The extreme differences are:

$$R(\tau) = \max_{1 \leq t \leq \tau} X(t, \tau) - \min_{1 \leq t \leq \tau} X(t, \tau) \quad \tau = 1, 2, 3, \dots, n \quad (5)$$

The standard deviations are:

$$S(\tau) = \left[ \frac{1}{\tau} \sum_{t=1}^{\tau} (\xi(t) - \langle \xi \rangle_{\tau})^2 \right]^{\frac{1}{2}} \quad \tau = 1, 2, 3, \dots, n \quad (6)$$

Where the following relationship is satisfied between R, S,  $\tau$  and H is the Hurst index:

$$\frac{R}{S} = \left( \frac{\tau}{2} \right)^H \quad (7)$$

The range of values of the Hurst coefficient H corresponds to three cases respectively (Pan et al. 2012): (1) when  $H=0.5$ , it means that the indicators are completely independent and there is no interdependence; (2) when  $0.5 < H < 1$ , it means that the time series has persistence or long-range correlation, implying that the future ozone trend is consistent with the past and the closer the value of H is to 1, the stronger the persistence is; (3) when  $0 < H < 0.5$ , it means that the future overall trend is opposite to the past and is resistant to persistence and the closer the H value is to 0, the stronger the resistance to persistence [15-20].

## 4. Results and Discussion

### 4.1 Spatial Distribution of Tropospheric Ozone Concentrations in the Horqin Grassland

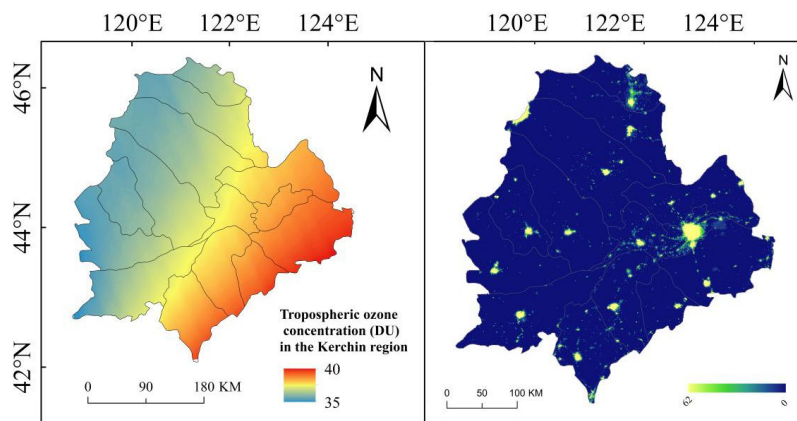


Figure 2: Map of interannual spatial variation of tropospheric ozone and spatial distribution of nighttime light in the Horqin Grassland region

The spatial distribution of the 8-year average annual ozone column concentration was obtained by processing the tropospheric ozone column concentration data in the Horqin Grassland region from 2013 to 2020 (Fig. 2). Figure 2 shows that, in terms of spatial distribution, the ozone column concentration in Horqin has prominent zonal distribution characteristics. Overall, the distribution pattern gradually increases from the west to the east. DMSP/OLS night lighting is an essential branch of the remote sensing application field. The DN value of the image element represents the average light intensity at night, which can indirectly reflect the characteristic information of urbanization level, traffic roads, and population concentration. We are analyzing the presence or absence of anthropogenic impacts on ozone based on

light intensity distribution at night. As shown in Fig. 2, the nighttime light DN values are unevenly distributed in the Horqin area, but the DN values are higher in the eastern part of Horqin. It is mainly concentrated in Tongliao City, and the DN values in the western region are relatively low and scattered. As can be seen from Figure 2, there is a relative consistency between areas of high ozone values and areas of high DN values. It indicates that the areas with higher DN values of lights at night are also areas with relatively higher concentrations of ozone columns. Increased light intensity may increase column ozone concentrations in the corresponding area. Meanwhile, the industry is one of the essential pillar industries in Tongliao City, mainly focusing on coal, electric power, iron and steel, chemical industry, machinery manufacturing, and building materials. This results in higher levels of ozone precursor pollutants such as particulate matter and nitrogen oxides in the area, which is favorable for ozone production, and therefore, the area is prone to be a high ozone value area [21-23].

#### 4.2 Mean annual distribution of tropospheric ozone in the Horqin Grassland area

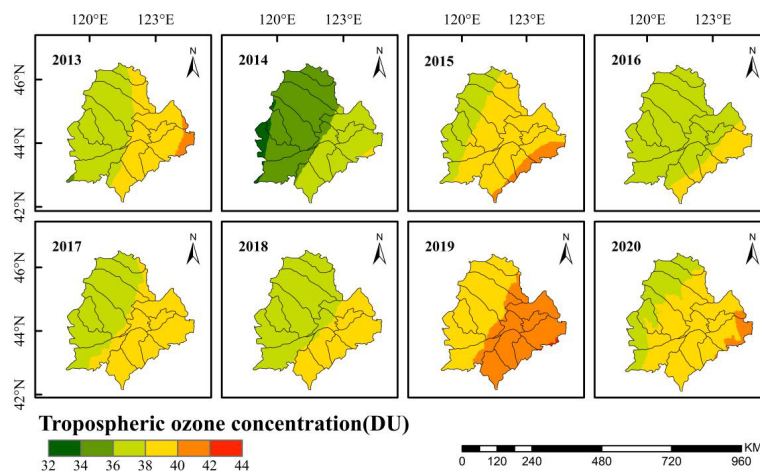


Figure 3: Interannual spatial variability of tropospheric ozone in the Horqin Grassland region

The tropospheric ozone column concentrations in the Horqin region from 2013 to 2020 can be classified into six levels (Figure 3): level 1, 32-34 DU; level 2, 34-36 DU; level 3, 36-38 DU; level 4, 38-40 DU; level 5, 40-42 DU; and level 6, 42-44 DU. As shown in Figure 3, the ozone column concentration values showed a gradually increasing distribution trend from the northwest to the southeast. In general, the high ozone column concentration area is distributed in the southeast of the Horqin region, mainly in the left wing of Horqin and Tongliao City. The lowest values are distributed around Bahrain Right Banner and Wengniuet Banner, while other areas form a transition zone. In these eight years, the concentration values were low in 2014, relatively stable in the ozone level distribution from 2016-2018, and began to increase after 2019 and were the highest in 2019 among the eight years.

#### 4.3 Analysis of tropospheric ozone concentration in the Horqin Grassland region based on image metric trends

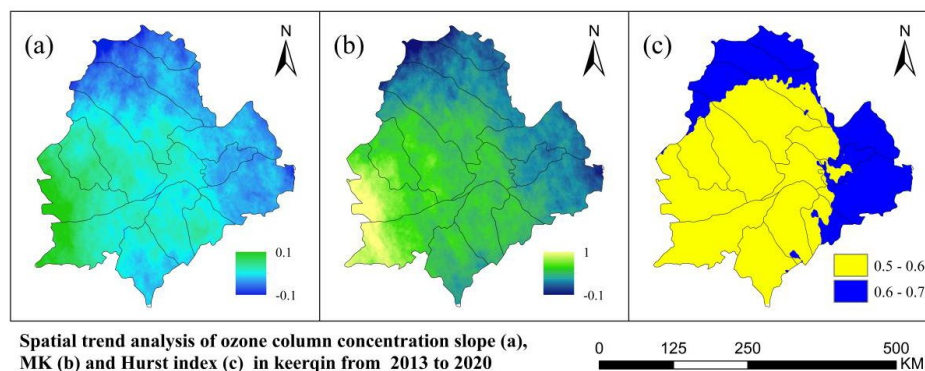


Figure 4: Spatial distribution of slope of ozone concentration trend (a), MK (b) and Hurst index (c), 2013-2020

As shown in Fig. 4a, the slope of the ozone trend in the Horqin region is indicated. Figure 4b shows

the MK of the overall concentration of the tropospheric ozone column in the Horqin region. Figure 4c shows the distribution of the ozone Hurst index. Since MK can only characterize changes in the increasing or decreasing ozone column concentrations trend, univariate linear regression analysis (slope) was used to calculate the change in specific slope ( $\theta$ ). Both MK and slope were calculated at the 95% confidence level.  $MK < 0$  is distributed in the northernmost part of the right-wing of Horqin and the eastern part of the left wing of Horqin. 99.68% of the overall study area is covered by  $MK > 0$ , indicating that tropospheric ozone concentration is increasing in most of Horqin. At the same time, the mean value of the slope of change of tropospheric ozone concentration in the Horqin area is 0.01. This shows that the concentration values have shown an upward trend at the end of the last eight years, but the increasing trend is insignificant. Among them, the rise in ozone concentration was more evident in Bahrain Right Banner and Wengniuet Banner. The ozone concentration ozone levels in other places were relatively stable with an insignificant increasing trend. The Hurst index in the Kerchin region showed weak persistence, indicating that ozone concentration will increase with future development in the region. The persistence of past trends in concentration values is more vital in the northern and eastern parts of the study area, accounting for 31.98% of the overall study area. Therefore, there is a need to strengthen the daily monitoring of the area, which will help assist the relevant authorities in formulating air management programs and provide better insight into the changes in pollutant concentrations.

#### 4.4 Analysis of tropospheric ozone concentration in the Horqin Grassland region based on image metric trends

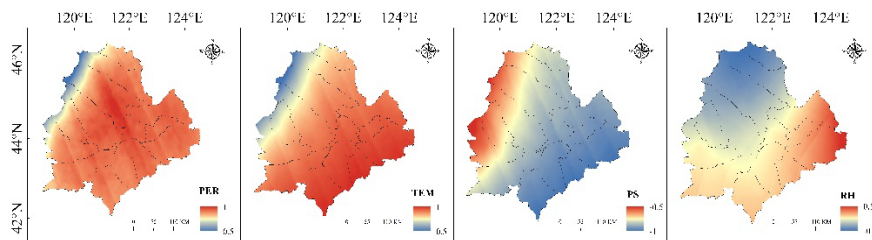


Figure 5: Trend plot of linear regression of Pearson's correlation between ozone and meteorological factors

Atmospheric pollutants have a specific solubility in water. The effects of water quality on ozone column concentration were analyzed in terms of precipitable water and relative humidity, respectively. As can be seen from Figure 5, the mean value of the regression coefficient for the correlation between ozone and precipitable water in the Horqin grassland area is 0.8625, and the correlation is relatively low in the northwestern part of the right wing of the huqin and Zalut banners. The relative humidity-ozone correlation was predominantly negative, with a mean regression coefficient of around -0.23 and a negative correlation area of 99.4% of the overall study area. Relative humidity affects the dilution and deposition of ozone, thus reducing the column ozone concentration. The areas with a positive correlation with ozone concentration values were mainly distributed in the eastern part of the left wing of Horqin. Temperature reflects the intensity of solar radiation, which directly correlates with ozone production and affects the photochemical reaction rate to some extent (Bai, 2001). High temperature promotes ozone production, and the regression coefficients of temperature ranged from 0.6852 to 0.8640. The temperature has less effect on ozone in the eastern part of Zarut Banner, Aluqorqin, Bahrain Left Banner, and Bahrain Right Banner. In terms of the overall study area, the effect of barometric pressure on ozone showed an overall negative correlation. In the eastern part of Horqin, where ozone concentration values are lower, the negative effect of air pressure on ozone is smaller. The mean value of the regression coefficient between air pressure and ozone concentration values was -0.874[24-28].

## 5. Conclusions

Regarding spatial distribution, the ozone column concentration in Horqin has prominent zonal distribution characteristics. The overall distribution pattern gradually increased from the west to the east. The nighttime light DN values were higher in the eastern part of Horqin, mainly concentrated in Tongliao City.

In the inter-annual variation, the ozone column concentration values gradually increased from the northwest to the southeast. Among the eight years, the concentration value in 2014 was lower, while the concentration value in 2019 was the highest among the eight years.

The MK of the overall tropospheric ozone column concentration and the slope of the trend of change in the Horqin region yielded that the ozone concentration is increasing, but the growth trend is not significant. The weak persistence from the Hurst index indicates that the ozone concentration will increase with the region's future development.

From the correlation analysis between ozone and natural factors, it can be seen that there is a good positive correlation between ozone and precipitable water but a negative correlation with relative humidity in the 99.4% region. High temperature promotes ozone production with regression coefficients ranging from 0.6852 to 0.8640. Air pressure has less negative effect on ozone in the eastern part of Horqin, where ozone concentration values are lower.

### Acknowledgement

**Funding:** This work was supported by the Natural Science Foundation of Gansu Province (CN)(17YF1FA120) at the Key Laboratory of Resource Environment and Sustainable Development of Oasis, Gansu Province.

**Author Contributions:** The author of this paper is Jinyang Wang, the first author, mainly responsible for data collection and processing, mapping, analysis and discussion, and paper writing. The responsible author is Professor Tianzhen Ju, who is mainly responsible for the topic selection and writing guidance. The co-author is Bingnan Li, who is mainly responsible for the guidance and language polishing of the paper. The other co-authors, Shengtong Lei, Shuai Peng were mainly responsible for formatting and paper fluency.

**Data Availability:** All data generated or analyzed during this study are included in this published article and its supplementary information files.

### References

- [1] Curci G., Palmer P. I., Kurosu T. P., Chance K., Visconti G.. *Estimating European volatile organic compound emissions using satellite observations of formaldehyde from the Ozone Monitoring Instrument [J]. Atmospheric Chemistry and Physics*, 2010, 10(215).
- [2] Deng Xuejiao, Zhou Xiuji, Wu Tui et al. *Influence of atmospheric aerosols on ground-level ozone changes in the Pearl River Delta [J]. Science China: Earth Science*. 2011, 41(1): 93-102.
- [3] Hu M, Deng Z, Wang Y et al. *Comparison of membrane sampling for offline analysis and online determination of elemental and organic carbon in atmospheric fine particles [J]. Environmental Science*. 2008, 29(12): 3297-3303.
- [4] Huang, R., Ju, T., Dong, H., Duan, J., Fan, J., Liang, Z., Geng, T. (2021). *Analysis of atmospheric SO<sub>2</sub> in Sichuan-Chongqing region based on OMI data [J]. Environmental monitoring and assessment* 193(12): 849 doi: <https://doi.org/10.1007/s10661-021-09638-2>.
- [5] JIANG Weifang, CAI Chenxia, LI Xin. *Modelling of ozone production in the urban lower atmosphere [J]. Meteorological Science*. 2001, 21(2): 154-161.
- [6] Jianhui B, Mingxing W. *The Primary Study on the Regularity of Atmospheric Photochemical Process for Surface Ozone [J]. Climatic and Environmental Research*, 2001. <https://ks.cqvip.com/Qikan/Article/Detail?id=5182999>
- [7] Zong Xuemei, Wang Gengchen, Chen Hongbin et al. *Characterisation of atmospheric ozone concentration changes in the boundary layer of Beijing [J]. Environmental Science*. 2007, 28(11): 2615-2619.
- [8] LI Yang, CHANG Limin, LU Peicheng, YANG Yamei, WANG Zhanshi, GE Huiping, GAO Hong, HUANG Tao, MA Xiaoxuan, MA Jianmin. *Sensitivity analysis of atmospheric ozone generation in Lanzhou City and its precursor emission reduction countermeasures [J]. Journal of Environmental Science*, 2021, 41(05): 1628-1639.
- [9] LU Xiujuan, JU Tianzhen, XIE Shuntao, GUO Meiyong, ZHANG Xue, ZHANG Hui'e, ZHANG Shengcai. *Study on the temporal and spatial variations of atmospheric ozone and influencing factors in Lanzhou [J]. Earth and Environment*, 2018, 46(04): 355-363.
- [10] LI Yang, JU Tianzhen, MA Cheng, CHANG Feng, ZHANG Yanping, HE Fan, WANG Qingqing. *Changes of formaldehyde column concentration and influencing factors in the Yangtze River Delta in the last 10 years [J]. China Environmental Science*, 2019, 39(03): 897-907.
- [11] Lu W.H. *Research on IDL Language Processing of Remote Sensing Data in HDF Format [J]. Marine Information*, 2006(03): 6-7.

- [12] Ma, C. et al. (2020). Spatiotemporal variations of tropospheric NO<sub>2</sub> in Lanzhou for the period 2009-2018 based on satellite remote sensing[J]. *Atmospheric Pollution Research*, 12(2):206-216. <https://doi.org/10.1016/j.apr.2020.11.003>.
- [13] Pan S, Choi Y, Roy A, et al. 2017. Allocating emissions to 4 km and 1 km horizontal spatial resolutions and its impact on simulated NO<sub>x</sub> and O<sub>3</sub> in Houston, Tx. *Atmospheric Chemistry and Physics*.
- [14] Pan YJ, Wang YL, Peng J, Shen H, Liu SQ (2012) Time series analysis of precipitation in the middle and lower reaches of Han River basin based on wavelet and R/S methods[J]. *Geography Research* 31(05):811-820
- [15] Peng S, Ju T, Liang Z, Li M, Liu S, Pan B (2022) Analysis of atmospheric ozone in Fenwei Plain based on remote sensing monitoring. *Environ Monit Assess* 194, 412 doi:<https://doi.org/10.1007/s10661-022-10082-z>
- [16] QU Yu, AN Junling. Contributions of anthropogenic and biogenic emissions to ozone - an example from East Asia in spring and summer[J]. *China Environmental Science*. 2009,29(4):337-344.
- [17] Ran L, Zhao C S, Xu W Y, et al. VOC reactivity and its effect on ozone production during the HaC hi summer Campaign[J]. *Atmospheric Chemistry and Physics*. 011, 11(10): 8595-8623.
- [18] SAN Wenpo, YIN Yongquan, DU Shiyong et al. Factors affecting urban atmospheric O<sub>3</sub> concentration in summer and their correlations[J]. *Environmental Science*. 2006,27(7):1276-1281.
- [19] Senff C J, Alvarez R J, Hardesty, et al. 2010. Airborne lidar measurements of ozone flux downwind of Houston and Dallas[J] *Journal of Geophysical Research*, 115:D20307
- [20] TANG Xiaoyan, ZHANG Yuanhang, SHAO Min. *Atmospheric Environmental Chemistry (Second Edition)* [M]. Beijing: Higher Education Press. 2006.
- [21] WANG Xuesong, LI Jinlong. A case study of ozone source identification in Beijing[J]. *Journal of Peking University (Natural Science Edition)*. 2003,39(2):244-253.
- [22] Wang XL, Hu BQ, Xia J (2002) R/S analysis method for hydrological time series trends and variation points [J]. *Journal of Wuhan University (Engineering Edition)* (02):10-12
- [23] Xu, J., Lu, Y. M. (2021). A OMI data based on the China regional tropospheric O<sub>3</sub> inversion method [J]. *Journal of Nanjing Information Engineering University (Natural Science Edition)*, 13(6):707-719. The DOI: 10.13878/j.carol carroll nki jnuist. 2021.06.009.
- [24] XU Xiaobin, LIN Weili, WANG Tao et al. Trends of tropospheric ozone in the Yangtze River Delta region[J]. *Progress in Climate Change Research*. 2006,2(5):211-216.
- [25] Xie X, Shao M, Liu Y et al. Daily variation characteristics of atmospheric volatile organic compounds (VOCs) and their roles in ozone generation - A case study of Guangzhou in summer[J]. *Journal of Environmental Science*. 2009,29(1):54-62.
- [26] YIN Yongquan, LI Changmei, MA Guixia et al. Distribution characteristics of urban ozone concentration[J]. *Environmental Science*. 2004,25(6):16-20.
- [27] ZHANG Yuanhang, SHAO Kesheng, TANG Xiaoyan et al. Photochemical smog pollution in Chinese cities[J]. *Journal of Peking University (Natural Science Edition)*. 1998,34(Z1):260-268.
- [28] ZHU Shuai, MA Jianzhong, WANG Yan et al. Numerical modelling of anomalously high spring ozone values in the Yangtze River Delta[J]. *Environmental Science Research*. 2006,19(6):1-8.